Kinetic Refolding Barrier of Guanidinium Chloride Denatured Goose δ-Crystallin Leads to Regular Aggregate Formation

Fon-Yi Yin,* Ya-Huei Chen,† Chung-Ming Yu,‡ Yu-Chin Pon,† and Hwei-Jen Lee†
*Department of Biology and Anatomy, and †Department of Biochemistry, National Defense Medical Center, Taipei, Taiwan; and ‡Institute of Biological Chemistry, Academia Sinica, Taipei, Taiwan

ABSTRACT δ-Crystallin is the major soluble protein in avian eye lenses with a structural role in light scattering. Dissociation and unfolding of the tetrameric protein in guanidinium chloride (GdmCl) can be sensitively monitored by the intrinsic tryptophan fluorescence. In this study refolding of GdmCl-denatured δ-crystallin was investigated. A marked hysteresis was observed while refolding by dilution of the 5 M GdmCl-denatured δ-crystallin. The secondary structure of the refolded protein was largely restored. However, monitoring intrinsic fluorescence of single tryptophan mutants indicated that the microenvironment of domain 1 (W74) was not restored. The region containing W169, which is close to the dimer interface, remained exposed following refolding. During refolding of the wild-type protein, dimeric, tetrameric, and aggregate forms were identified. The ratio of tetramer to dimer increased with time, as judged by gel-filtration chromatography and nondenaturing gel electrophoresis. However the observed levels of tetramer did not return to the same levels as observed before GdmCl treatment. The proportion of tetramer was significantly decreased in the N-25 deletion mutant and it did not increase with time. These results suggest that there is a kinetic barrier for assembly of dimers into tetramers. The consequence of this is that dimers refold to form aggregates. Aggregation seems to follow a nucleation mechanism with an apparent reaction order of 4.7 ± 0.2, suggesting four or five monomers constitute the core structure of nucleus, which propagate to form high molecular weight aggregates. Addition of α-crystallin during refolding prevents aggregation. Thioflavin T and Congo red assays indicated a regular structure for the protein aggregates, which appear as hollow tubules packed into helical bundles. Aggregate formation was protein concentration dependent that progressed via two stages with rate constants of 0.0039 ± 0.0006 and 0.00043 ± 0.00003 s^{-1}, respectively. We propose that the N-terminal segment of δ-crystallin plays a critical role in proper double dimer assembly and also in the assembly of nucleus to aggregate formation.

INTRODUCTION

Eye lens is a specialized tissue required for vision, with the nuclei and organelles of cells depleted after maturation to reduce light scattering. Crystallins are the main lens proteins, which are highly stable and water soluble and play a key role in determining and maintaining the refractive index of the lens (1). α-, β-, and γ-Crystallin are known as ubiquitous crystallins, and are widely distributed in all vertebrate species. Other crystallins, which are found only in certain taxon species, share highly sequence homologies with some metabolic enzymes (2,3). Examples of these enzymes/crystallins include δ-crystallin/argininosuccinate lyase (ASL) and ε-crystallin/lactate dehydrogenase in birds and reptiles; η-crystallin/aldehyde dehydrogenase in elephant shrews; S-crystallin/glutathione S-transferase and Ω-crystallin/aldehyde dehydrogenase in octopi; and ξ-crystallin/NADPH:quinone oxidoreductase in guinea pigs. The significance of the evolutionary relationship between these crystallins and housekeeping enzymes is unclear. However, it is believed that it is necessary for the lens to acquire proteins that are thermodynamically stable and are able to accumulate at high levels in sensitive environments and limited space (4).

δ-Crystallin is a tetrameric protein sharing ~70% sequence identity with argininosuccinate lyase (1,5). The structures of δ-crystallin and related proteins have been determined (6–9). They share similar overall topology and exist as a dimer of dimers. Each monomer in the structure contains 19 α-helix and eight β-strands and is divided into three domains. Domain 2, which contains five helices, associates with other subunits to form the core 20-helix bundle that constitutes the major part of the protein (Fig. 1 *A*). Neighboring subunits interact to form the closely associated dimer in which domain 1 of one subunit interacts with domain 3 of the other subunit. Two kinds of the dimers are then assembled to form the tetramer. In this structure the N-terminal segment interacts with a hydrophobic cavity in a neighboring molecule, stabilizing the quaternary structure (Fig. 1 *B*). Therefore, truncation mutants have an impaired double dimer assembly process (9).

δ-Crystallin is equilibrium unfolded in guanidinium chloride (GdmCl) in a multiple step unfolding mechanism, which includes subunit dissociation and formation of a molten

Submitted January 16, 2007, and accepted for publication April 6, 2007.

Address reprint requests to Dr. Hwei-Jen Lee, Dept. of Biochemistry, National Defense Medical Center, No. 161, Sec. 6, Minchuan East Rd., Neihu, Taipei 114, Taiwan. Tel.: 886-2-87910832; Fax: 886-2-87923106; E-mail: hjlee@mail.ndmctsgh.edu.tw.

Abbreviations used: ASL, argininosuccinate lyase; ANS, 1-anilinonaphthalene-8-sulfonic acid; GdmCl, guanidinium hydrochloride; N-25, deletion of 25 residues from the N-terminus of goose δ-crystallin; ThT, thioflavin T; CR, Congo red; TEM, transmission electron microscopy.

Editor: Heinrich Roder.

0006-3495/07/08/1235/11 $2.00

doi: 10.1529/biophysj.107.104604

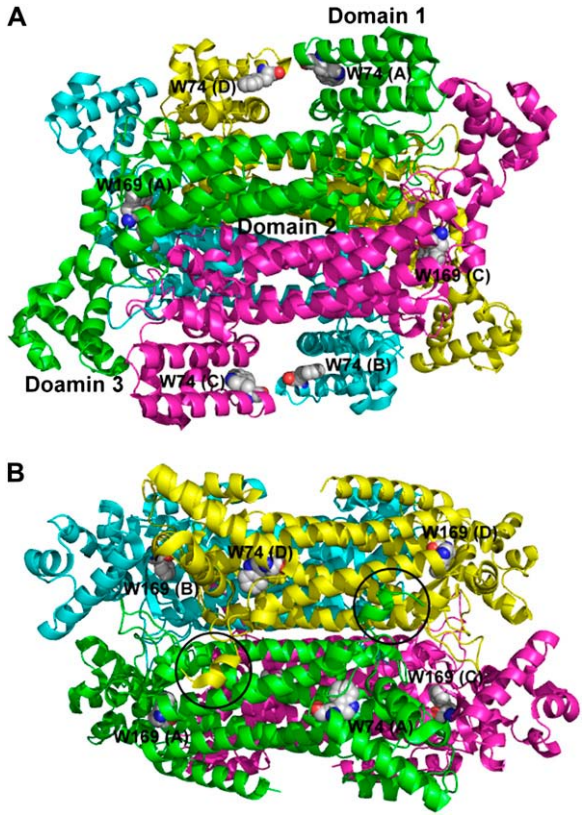

FIGURE 1 Ribbon diagrams of the goose δ-crystallin tetramer (Protein Data Bank accession code 1XWO). Panels *A* and *B* represent the same structure rotated by 90° about the horizontal axis. Subunits A, B, C, and D were shown in green, cyan, magenta, and yellow, respectively. Residues of W74 and W169 were shown by spheres. Circles in panel *B* depicted the protruded N-terminal arm to the neighboring subunit.

globule intermediate (10,11). The subunit dissociation step can be sensitively monitored by tryptophan fluorescence. We have demonstrated that both tryptophan residues of δ-crystallin, W169 and W74, are sensitive indicators of GdmCl-induced denaturation (12). Disruption of interactions contributed by W169 in the helix bundles further destabilizes the protein conformation and makes the protein prone to disassembling the tetramer.

Dilution of denatured δ-crystallin in 5 M GdmCl allows protein refolding, and can be followed by the blue shift in the fluorescence spectrum of the protein. The fluorescence intensity, however, was not restored (10). This prompted us to further investigate the fluorescence quenching of this tryptophanyl residue. Chemical denaturant unfolded protein can be refolded spontaneously in the absence of any additional molecular species (13). However, due to the lack of a favorable folding environment, many large proteins might not be successfully refolded in vitro even in the presence of assisting chemicals or chaperones (14). Under such conditions, the competing aggregation event is the predominant process. Competition of an aggregation pathway with the refolding process of the GdmCl-denatured protein has been demonstrated in a number of different studies, e.g., human γ-crystallin (15), human muscle creatine kinase (16), lactate dehydrogenase (17,18), and transthyretin (19). Protein aggregation is related to many pathogenic conditions in vivo, with most common protein-misfolding diseases characterized by deposit of amyloid fibrils within or outside of the cells (20–22).

Previously, we have reported a pH-induced reversible dissociation of duck δ2-crystallin (23). However, the detail mechanism of the refolding of denatured polypeptide chain remains unknown. This study is aimed at identifying intermediates that lead to native-like protein species during refolding. Aggregation was also investigated to determine whether this process competes with refolding of GdmCl-denatured goose δ-crystallin. The results revealed that when GdmCl-denatured protein was diluted, denatured δ-crystallin subunits were able to refold and reconstitute dimers. However, further assembling into double dimeric tetramers is rate-limiting and this increases the possibility of aggregate formation. The N-terminal segment in the structure is critical for both double dimer assembly and also in delaying aggregate formation. Characteristic tubular α-helical bundles were shown to be formed in protein aggregates by transmission electronic microscopy (TEM). We proposed an alternative subunit association model to explain the formation of high molecular weight aggregates.

EXPERIMENTAL PROCEDURES

Materials

All chemicals were of analytic grade or higher and were obtained from Sigma-Aldrich (St. Louis, MO) or Fisher (Leicestershire, UK) unless otherwise stated. Enzymes for molecular biology procedures were obtained from New England Biolabs (Beverly, MA). Chromatography systems and columns were supplied by GE Healthcare (Fairfield, CT). Mutants of goose δ-crystallin with N-terminal truncation, W74F, and W169F were prepared as previously reported (9,12).

Protein expression and purification

δ-Crystallin was purified as reported previously (9). Briefly, clones of wild-type or mutant *pET*-gδ gene were expressed in *Escherichia coli* BL21 (DE3) with induction by isopropyl-β-D-thiogalactopyranoside. After incubation for 16 h at 27°C, cells were harvested by centrifugation and kept frozen at −80°C. Protein concentrations were determined by the protein-dye binding method of Bradford using bovine serum albumin as the standard (24).

The frozen cells were resuspended and sonicated in buffer A (50 mM Tris-HCl buffer, pH 7.5). The supernatants were loaded onto a Q-Sepharose anion exchange column (HiPrep 16/10 Q XL, Amersham Bioscience, Uppsala, Sweden) preequilibrated in buffer A and eluted with a linear gradient of 0–0.3 M NaCl in buffer A. Recombinant goose δ-crystallin was eluted at ~0.12 M NaCl. Ammonium sulfate fractionation was performed on the pooled fractions. The 40 ~ 50% (w/v) saturation pellets were dissolved in 5 ml buffer A and loaded onto a S-300 Sephacryl column (26 mm × 85 cm) preequilibrated in buffer A. The highest purity fractions were pooled and concentrated.

Porcine lens α-crystallin was purified from fresh porcine eye balls. The filtered supernatant sample after homogenization was loaded into a TSK

HW55 gel filtration column that has been equilibrated with elution buffer (10 mM Na_2HPO_4, 2 mM KH_2PO_4, 3 mM KCl, 5 mM EDTA, and 1.4 mM 2-mercaptoethanol, pH 7.4). The fractions containing α-crystallin after SDS-PAGE analysis were pooled and frozen at −80°C.

Fluorescence studies

The fluorescence spectra of δ-crystallin were measured in a Perkin-Elmer LS-50 luminescence spectrophotometer (Foster City, CA) equipped with a thermostatically controlled sample holder. Intrinsic tryptophan fluorescence spectra of the protein were recorded with excitation wavelength set at 295 nm and band widths of 5 nm for both excitation and emission wavelength. Equilibrium unfolding experiments was performed by incubating δ-crystallin with various concentrations of GdmCl in 0.1 M Tris-HCl buffer, pH 7.5, at 25°C overnight. All spectra were corrected for buffer or GdmCl absorption. The refolding experiments were undertaken by 20-fold dilution of 5 M GdmCl-denatured δ-crystallin into a series of different GdmCl concentrations.

To consider both the variation in the red shifting and fluorescence intensity, the average emission wavelength method was utilized for data analysis (25): $\langle\lambda\rangle = \sum_{i=\lambda_1}^{\lambda_N}(F_i \times \lambda_i)/\sum_{i=\lambda_1}^{\lambda_N} F_i$, where $\langle\lambda\rangle$ is the average emission wavelength and F_i is the fluorescence intensity at the emission wavelength of λ_1.

Protein conformational change was accessed by the binding ability with 0.2 mM ANS (1-anilinonaphthalene-8-sulfonic acid) (Molecular Probes, Eugene, OR), whose fluorescence spectrum was recorded from 450 to 550 nm with the excitation wavelength set at 370 nm.

Circular dichroism studies

Circular dichroism (CD) spectra were obtained by using a Jasco (Tokyo, Japan) J-810 spectropolarimeter with a thermostatically controlled sample holder. Experiments were performed in 10 mM sodium phosphate buffer (pH 7.0) using 0.1 cm pathlength cell for the far-ultraviolet (UV) region (200–250 nm). All spectra were averaged from three accumulations and were buffer corrected. The mean residue ellipticity $[\theta]$ was calculated according to $[\theta] = \theta M_{MRW}/10dc$ (26), where θ is the observed ellipticity (degrees), M_{MRW} is the mean residue weight, in which for goose δ-crystallin is 110.5 g/mol, d is the light path (cm), and c is the concentration of protein in g/ml.

Nondenaturing gradient gel electrophoresis

Electrophoresis was performed with PhastGel 4-1 5% gradient gel and Native Buffer Strip (containing 0.88 M *L*-alanine, 0.25 M Tris-HCl, pH 8.8) on the PhastSystem (GE Healthcare). The samples were subjected to electrophoresis at 10 mA at 15°C for 400 Vh. After electrophoresis the gel was fixed in 20% (w/v) trichloro-acetic acid and stained with Silver Stain (Bio-Rad, Hercules, CA).

Analytical gel-filtration chromatography

The wild-type and mutant δ-crystallin were analyzed by gel-filtration chromatography (ÄKTA FPLC system, GE Healthcare, Tokyo, Japan) using a Superdex 200 HR 10/30 column. The supernatant of centrifuged protein samples were injected into the column preequilibrated with buffer A. The column was calibrated with proteins of known M_r under the same conditions.

Refolding kinetics

Protein refolding kinetic was monitored by direct dilution of the 5 M GdmCl-denatured δ-crystallin with buffer A. The fluorescence intensity was measured with excitation and emission wavelengths set at 295 and 340 nm, respectively. The kinetic data were analyzed by fitting the increasing fluorescence intensity to exponential Eq. 1 and decreasing fluorescence intensity to Eq. 2 (27):

$$F_t = F_\infty + \sum_{i=1}^{n} F_i[1 - \exp(-k_i t)] \quad (1)$$

$$F_t = F_\infty + \sum_{i=1}^{n} F_i \exp(-k_i t), \quad (2)$$

where F_t is the signal at time t, F_∞ is the signal of the final state, n is the number of kinetic phases, F_i is the change in amplitude of each kinetic phase, and k_i is the rate constant for refolding. Data fitting was carried out using the SigmaPlot program.

Protein solution turbidity was measured by light scattering, which was performed in a Perkin-Elmer λ40 UV/Vis spectrophotometer with the wavelength set at 360 nm. All measurements were corrected with proteins without GdmCl under the same conditions.

Congo red assay

Proteins were equilibrium unfolded in 5 M GdmCl and diluted and mixed with Congo red (CR) at a final dye concentration of 20 μM in buffer A. The dye was freshly prepared in 5 mM KH_2PO_4-NaOH, 150 mM NaCl, pH 7.4, and filtered through 0.2 μm filter before use. The absorption spectrum of the mixture was recorded from 400 to 700 nm on a Perkin-Elmer λ50 UV/Vis spectrophotometer and corrected for absorbance from buffer and protein (28).

Thioflavin T assay

The assay was performed in Perkin-Elmer LS-50 luminescence spectrophotometer with excitation wavelength set at 440 nm and the emission spectrum from 460 to 600 nm was scanned. Proteins unfolded in 5 M GdmCl were diluted and mixed with thioflavin T (ThT) in buffer A to a final dye concentration of 50 μM. The spectrum of ThT alone was recorded and subtracted from the protein-containing samples. The dye was fresh prepared in buffer A and filtered through 0.2 μm filter before use. The kinetics of aggregate formation was monitored by measuring the increase of fluorescence intensity at 480 nm. The time-dependent fluorescence data were fitted to Eq. 1 (29).

Transmission electron microscopy

Refolded protein solution (10 μl, 0.047 mg/ml) was applied to Formvar and carbon-coated nickel grid, blotted, negatively stained with 1% (w/v) uranyl acetate, washed, and air-dried. The samples were examined in a JEOL (Tokyo, Japan) JEM-1230 transmission electron microscope operating at an exciting voltage of 80 kV.

RESULTS

Protein conformation of the GdmCl-denatured and renatured goose δ-crystallin as revealed by fluorescence spectra

Differences in protein conformation between native and refolded goose δ-crystallin were investigated by intrinsic protein tryptophan fluorescence. Immediately after dilution of the GdmCl-denatured protein the maximum emission wavelength was at 336 nm. After 1 min the wavelength was blue-shifted to 334 nm and after 1-h incubation it was shifted to 330 nm, which is the same for native protein (Fig. 2 *A*).

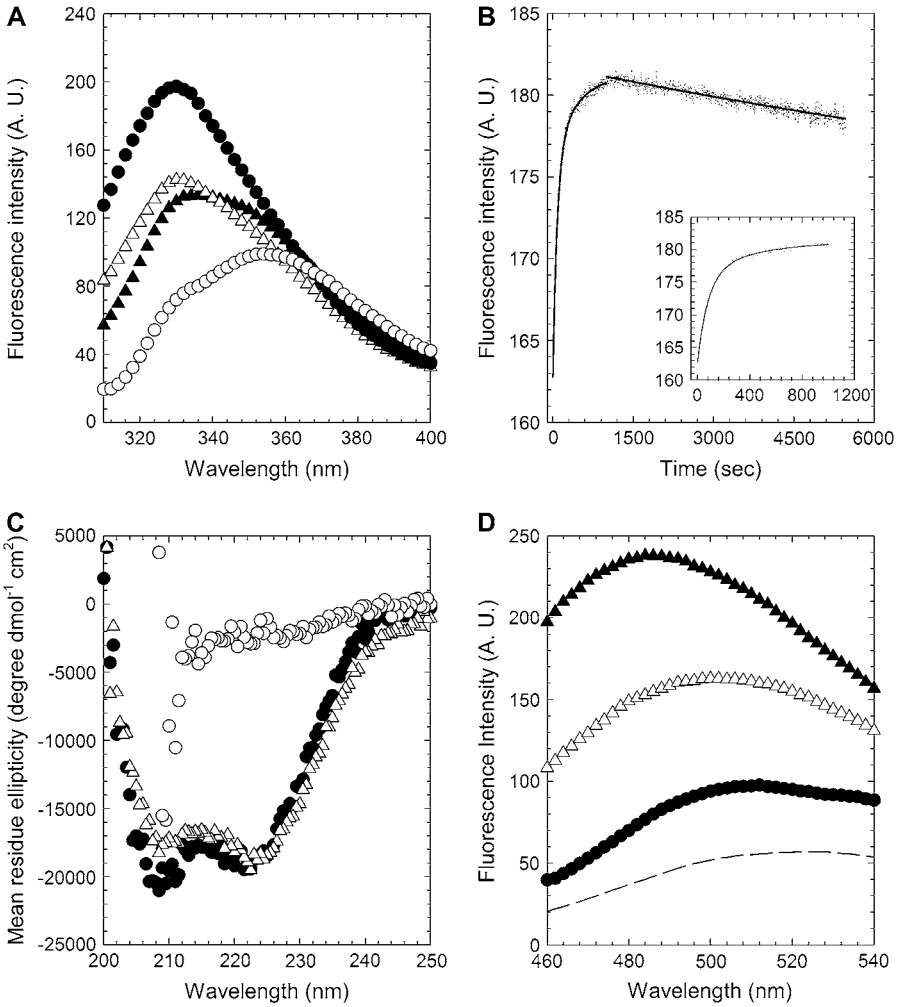

FIGURE 2 Time-dependent refolding of GdmCl-denatured δ-crystallin. δ-Crystallin (0.03 mg/ml), equilibrium denatured in 5 M GdmCl were 20-fold diluted with 50 mM Tris-HCl buffer, pH 7.5, and the intrinsic tryptophan fluorescence (*A*), far-UV CD (*C*), and ANS fluorescence (*D*), were analyzed at specific time, respectively. (*B*) Refolding kinetic traces of tryptophan fluorescence with dots are experimental data and the solid line represents the resulted fitting curve. Labels used in the figures are: solid circles (wild-type in 0.06 M GdmCl), open circles (wild-type unfolded in 5 M GdmCl), solid triangles (refolded wild-type at time zero), and open triangles (refolded wild-type after 1 h). Short dashed line in panel *C* represents the spectrum of ANS only.

However, the fluorescence intensity of the refolded protein was never fully restored to the original value, but was ~30% smaller than that of native protein (Fig. 2 *A*). Similar results have been previously reported for duck δ-crystallin, indicating that the refolded δ-crystallin assumed a native-like structure but was not in the same conformation as the native form (11).

Time-dependent refolding process as monitored by tryptophan fluorescence showed a burst of increasing fluorescence intensity at the onset followed by a gradual decrease (Fig. 2 *B*). The data for the increasing fluorescence were best fitted by a double exponential equation (Eq. 1), and for decreasing fluorescence were best fitted to single exponential equation (Eq. 2). A total of three rate constants were obtained (Table 1). Even within the limitations imposed by manual operation, two more refolding intermediates with $t_{1/2}$ of 46 and 301 s were detectable in the burst phase. Another slow transition with a half-life of 4.8 h was also observed in the decreasing fluorescence phase.

The secondary structure of the refolded protein was completely restored. Over 98% of the characteristic α-helical structure of δ-crystallin was restored after 1-h incubation (Fig. 2 *C*). However, exposure of the hydrophobic patches of the refolding protein detected by ANS showed a blue-shifted in wavelength and increased in fluorescence intensity after dilution for 1 h, longer time incubation did not improve further recovery in fluorescence intensity. The 10 nm shifted in wavelength and 40% difference in intensity compared

TABLE 1 Refolding kinetic measurements

Probe	[P] (mg/ml)	k_1 (s^{-1})	$t_{1/2}$ (s)	k_2 (s^{-1})	$t_{1/2}$ (s)	k_3 (s^{-1})	$t_{1/2}$ (s)
Fluorescence	0.024	0.015 ± 0.004	46 ± 12	0.0023 ± 0.0001	301 ± 13	0.00004 ± 0.00001	17328 ± 4332
ThT	0.035	0.0009 ± 0.00009	797 ± 82	–	–	–	–
	0.049	0.006 ± 0.0005	120 ± 10	0.0005 ± 0.00002	1507 ± 66	–	–

with those of the native protein indicate a different conformation for the refolded protein (Fig. 2 *D*).

GdmCl concentration dependent refolding of denatured goose δ-crystallin

To investigate the different conformations that can arise from refolding of GdmCl-denatured δ-crystallin, unfolding and refolding was measured at different GdmCl concentrations using intrinsic tryptophan fluorescence. The results showed that the transition curves for both unfolding and refolding were identical when GdmCl was >1 M for wild-type protein (Fig. 3 *A*). At concentrations of <1 M, the refolding curve showed a marked hysteresis behavior similar to that reported for transthyretin and γD-crystallin (30,15). It is interesting that the unfolding curve of the N-25 mutant protein coincided with the refolding curve of the wild-type protein. Since it has been previously reported (9) that the N-25 mutant is defective in double dimer (tetramer) formation, this suggests that the observed hysteresis in the wild-type protein is due to an asymmetrical dimer-tetramer interconversion. The average emission wavelength for the refolding transition when GdmCl concentrations were <1 M did not return to the original value for wild-type protein, implying a different tryptophan environment for the refolded proteins.

To assess the local microenvironment around individual tryptophan residues, refolding of single tryptophan mutants was studied. At GdmCl concentrations >0.8 M, the curves for unfolding and refolding of W74F mutant were similar. However, significant discrepancies in average emission wavelength were observed (Fig. 3 *B*). In the refolding curve the average emission wavelength blue-shifted from 356 to 342 nm, suggesting a partially buried microenvironment of W169. In contrast, the refolding curve for W74 remained unchanged after dilution of GdmCl, suggesting that the local environment of this residue is always relatively exposed.

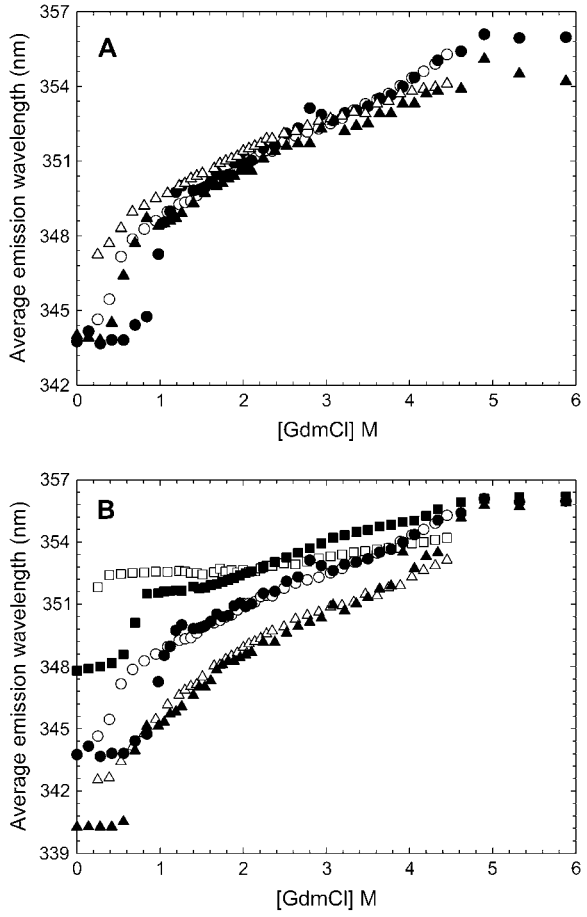

FIGURE 3 Refolding of GdmCl-denatured goose δ-crystallin. (*A*) Wild-type and N-terminal mutant (*B*) W74F and W169F mutants. All proteins after equilibrium denaturation were diluted to defined concentrations of GdmCl, and the fluorescence emission spectrum of tryptophan was measured. Protein concentration used in each assay was 0.05 mg/ml. Labels in the figure represent: solid circles (unfolding of wild-type), open circles (refolding of wild-type), solid triangles (unfolding of N-25 mutant in *A* and W74F mutant in *B*), open triangles (refolding of N-25 mutant in *A* and W74F mutant in *B*), solid squares (unfolding of W169F mutant) and open squares (refolding of W169F mutant).

Characterization of the hysteresis refolding of δ-crystallin

It has been previously reported that at GdmCl concentrations >∼1 M dissociation of the δ-crystallin tetramer occurs (10,11). To determine whether this dissociation is responsible for the observed hysteresis behavior, the oligomerization state of the protein was determined by gel filtration chromatography. Direct dilution of the GdmCl-denatured δ-crystallin resulted in two major peaks that were observed with elution volumes of 10.1 and 10.9 ml, corresponding to tetrameric and dimeric δ-crystallin, respectively (Fig. 4 *A*). For wild-type protein, the ratio between these two peaks increased from 0.45 to 1.5 after 2-h incubation in dilution buffer, and remained this ratio after 6-h incubation under the same conditions. The protein was precipitated after incubation for 20 h, suggesting misfolding and aggregation had occurred.

In the case of the N-25 mutant (Fig. 4 *B*) the major peak observed was at 11.1 ml, suggesting that dimer is the predominate species. The ratio of two peaks (10.1 and 11.1 ml) increased from 0.06 to 0.25 after 2-h incubation, indicating some formation of the tetramer or possibly formation of aggregation nuclei. Prolonging incubation also resulted in precipitation of protein (Fig. 4 *B*), suggesting that the latter process had taken place.

The heterogeneous nature of the refolded δ-crystallin was also demonstrated by nondenaturing gel electrophoresis (Fig. 5). For the wild-type protein, a distribution of dimer, tetramer, and aggregate appeared (Fig. 5 *A*). The tetramer/dimer ratio steadily increased from 0.76 to 2.5 after diluting refolding. In N-25 mutant δ-crystallin, only dimer and aggregate forms was observed, consistent with the results of gel filtration chromatography analyses (Figs. 5 *B* and 4 *B*).

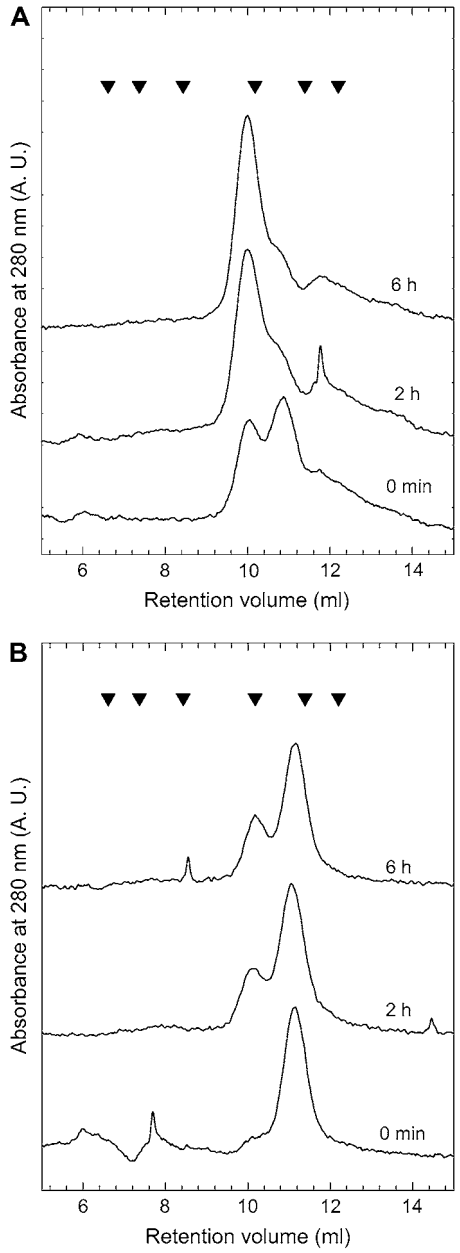

FIGURE 4 Time-dependent refolding of goose δ-crystallin traced by gel filtration chromatography. Wild-type (*A*) or N-25 mutant δ-crystallin (*B*) was equilibrium denatured in 5 M GdmCl and then diluted 20-fold with 50 mM Tris buffer, pH 7.5, for different time periods. The protein samples (0.13 mg/ml) were then injected into a Superdex 200 HR column for analysis. The M_r markers (*inverted solid triangles*) used were: (*from left to right*) blue Dextran (2000 kDa), thyroglobulin (669 kDa), ferritin (440 kDa), catalase (232 kDa), albumin (67 kDa), and ovalbumin (43 kDa).

It is noted for these minor bands that were shown in Fig. 5. The higher position than that of tetramer indicated that polymerization and aggregation would occur at the very early stage during refolding. The fraction of the refolded protein converted into the aggregates was determined by measuring the supernatant protein concentration at different time intervals. The refolded wild-type at the incubation of

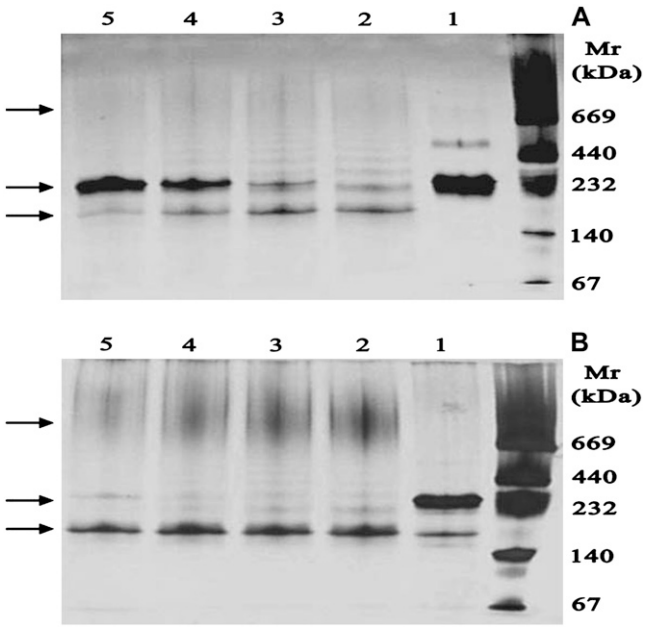

FIGURE 5 Time-dependent refolding transition of goose δ-crystallin traced by nondenaturing electrophoresis. Wild-type (*A*) or N-25 mutant δ-crystallin (*B*) was equilibrium denatured in 5 M GdmCl and then diluted 20-fold with 50 mM Tris-Cl, pH 7.5, for various time intervals. The protein samples (0.1 mg/ml) were then loaded on 4–15% gradient gels. (*Lane 1*) Protein without treatment with GdmCl. (*Lane 2*) Refolded at time zero. (*Lane 3*) Refolded for 30 min. (*Lane 4*) Refolded for 3 h. (*Lane 5*) Refolded overnight. Arrows shown from top to bottom showed the position of aggregates, tetramers, and dimers.

1 h, 6 h, or overnight led to the fractions of ~75%, 80%, and 95% of aggregates, respectively. And for N-25 mutant, it is ~60%, 75%, and 85%, respectively.

These results indicated several characteristics for the refolding process of δ-crystallin. Firstly, the dimeric form is an essential intermediate during the reassembly process. Secondly, the N-terminal region of goose δ-crystallin is critical in the assembly of the double dimer quaternary structure.

Aggregates formation kinetics on the refolding of δ-crystallin

Aggregation during refolding of denatured δ-crystallin was further analyzed by light scattering. The time-dependent increase of light scattering at 360 nm showed a sigmoidal curve with delay time that was correlated with protein concentrations (Fig. 6 *A*). There was a linear correlation for the log-log plot of δ-crystallin concentration versus reciprocal of delay time (t_d) with a slope of 4.7 ± 0.2, which represents the apparent reaction order. These conformed to a nucleation mechanism for the protein aggregates formation (Fig. 6 *B*) (31). For the N-25 mutant, the apparent reaction order was 4.3 ± 0.5. However, it should be noted that, as compared to wild-type protein, the N-25 mutant δ-crystallin

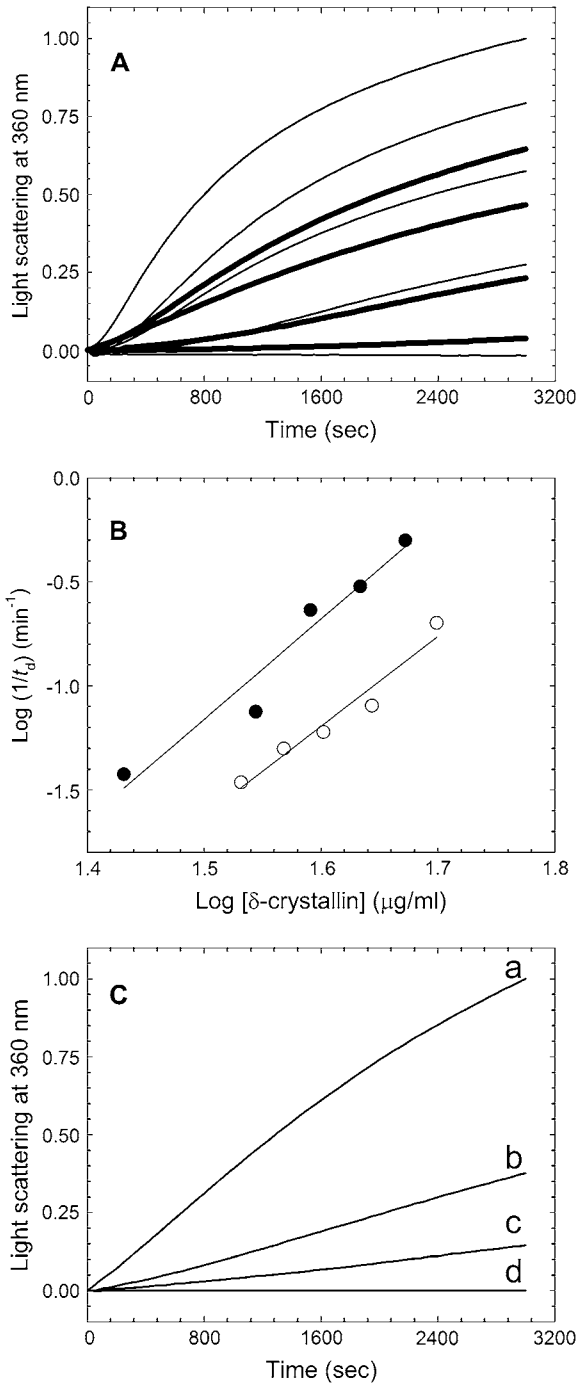

FIGURE 6 Light scattering of the aggregate formation during refolding of δ-crystallin. (*A*) Wild-type (*thin lines*) or N-25 mutant (*bold lines*) δ-crystallin, equilibrium denatured in 5 M GdmCl, were diluted into final concentration (*from top to bottom*) of 0.047, 0.043, 0.039, or 0.035 mg/ml, respectively. Time-dependent light scattering increase at 360 nm was recorded. Native δ-crystallin (0.047 mg/ml) without GdmCl was also shown (*bottom*). (*B*) Log-log plot of protein concentration versus delay time from panel *A*. Solid circles, wild-type; open circles, N-25 mutant. (*C*) Wild-type δ-crystallin (0.047 mg/ml) refolded in the (*a*) absence, or (*b*) presence of 0.15 and (*c*) 0.3 mg/ml of porcine lens α-crystallin. Light scattering of porcine lens α-crystallin itself (0.3 mg/ml) was shown in the bottom line (*d*).

took ~4 times longer to form aggregates and the reaction rate was reduced by 2.5-fold (Fig. 6 *A*). For the same measurement, no aggregates were observed for native δ-crystallin in the condition of 0.25 M GdmCl.

Light scattering from aggregate formation during the refolding of δ-crystallin was reduced by the addition of α-crystallin (Fig. 6 *C*). The formation of δ-crystallin aggregates was reduced by the presence of α-crystallin, presumably due to a delay in the onset of aggregation. α-Crystallin had a similar effect on aggregate formation for the N-25 mutant δ-crystallin (data not shown).

Structural features of the refolded δ-crystallin aggregates

Insoluble refolded δ-crystallin aggregates were visible at higher protein concentrations. To characterize the structural features of the aggregates, their binding abilities with ThT and Congo red dyes were examined. These two dyes have been extensively used to detect regular cross-β-structure of amyloid fibers (28,29). When mixed with δ-crystallin aggregates, the fluorescence of ThT increased obviously with an emission peak at 480 nm indicating binding between dye and the aggregates (Fig. 7 *A*). The time-dependent increase in fluorescence suggested increasing amounts of protein aggregates as detected by ThT binding. At [δ-crystallin] = 0.049 mg/ml the data were best described by a two-exponential kinetic reaction model, with the first and second rate constants calculated to be 0.006 ± 0.0005 and 0.0005 ± 0.00002 s^{-1}, respectively (Fig. 7 *C* and Table 1). When protein concentration was 0.035 mg/ml, a single exponential curve with a rate constant of 0.0009 ± 0.00009 s^{-1} described the results (Table 1). The fluorescence of aggregate bound ThT was not detectable at protein concentration lower than 0.03 mg/ml. N-25 mutant δ-crystallin also showed as a hyperbolic curve with similar rate constants for fibril formation, however, the whole process was delayed by a lag phase (Fig. 7 *C*).

δ-Crystallin aggregates were also detected by CR binding, as judged by the increase of protein-dye complex absorption spectra (Fig. 7 *B*). The absorption of CR increased in a time-dependent manner when binding with refolded δ-crystallin aggregates (Fig. 7 *D*). The absorption enhancement was fivefold more in wild-type protein than that of N-25 mutant. The increasing in the CR absorption must be due to interactions with δ-crystallin aggregates characteristic for this dye (32). It was thus intriguing to examine whether δ-crystallin has similar regular amyloid fibril structure found in many neurodegenerative disease (33,34).

The morphology of the refolded δ-crystallin aggregates was examined with transmission electron microscope. At the initial stage (~20 min), irregular spherical dark aggregates or chain-like structures were observed (Fig. 8 *A*). After 6 h of refolding, some unbranched fibril-like structures appeared with diameters of 46–61 nm, which then twisted into tubules composed of three strands with diameters ~108–123 nm

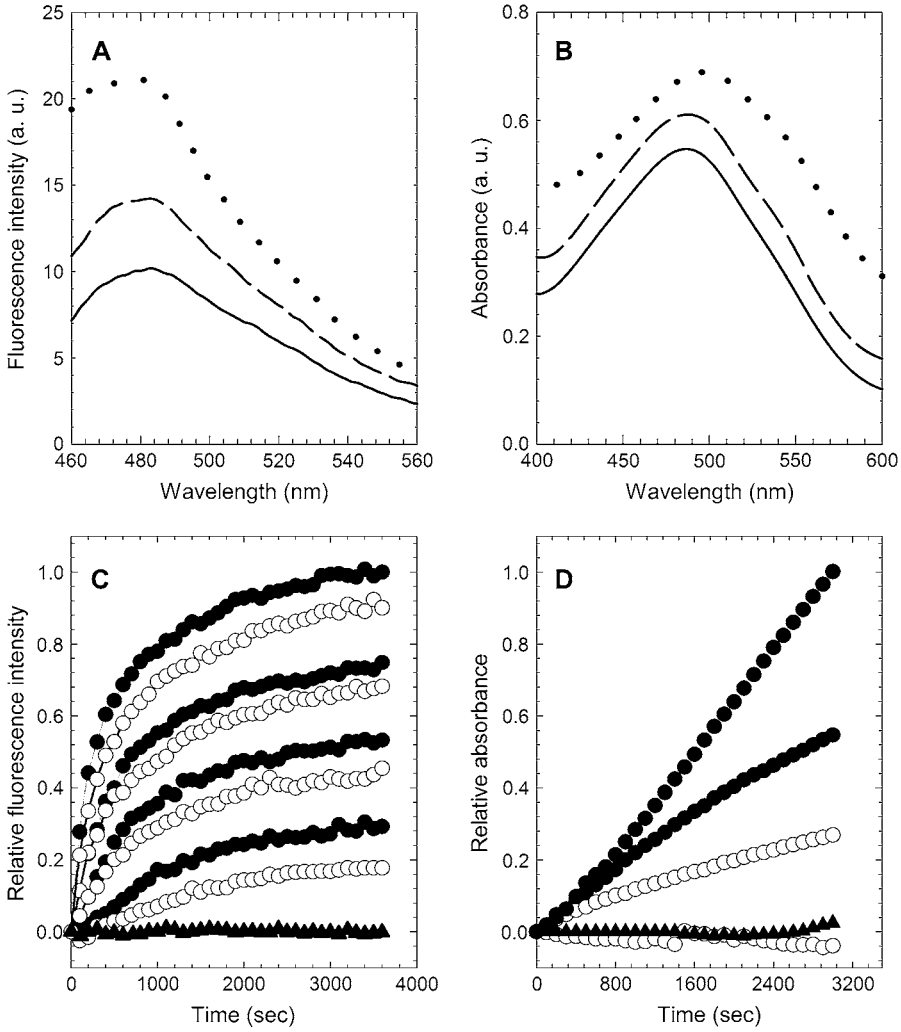

FIGURE 7 The ThT and CR assays. The spectrum of ThT (50 μM) (*A*) or CR (20 μM) (*B*) in the absence of (*solid line*) or in the presence of refolded wild-type δ-crystallin (0.05 mg/ml) at time zero (*dashed line*) or 1 h (*dotted line*) in 50 mM Tris-Cl buffer, pH 7.5. (*C* and *D*) Time course of fluorescence emission intensity at 480 or 550 nm for ThT and CR, respectively. Refolded wild-type (*solid circle*) or N-25 mutant (*open circle*) were analyzed in final diluted protein concentration (*from top to bottom*) of 0.047, 0.043, 0.039, or 0.035 mg/ml, respectively. Protein without GdmCl treatment was shown as control in the bottom line (*solid triangle*).

(Fig. 8, *B* and *C*). More extended and juxtaposed tubules with diverse length and diameter were produced after overnight incubation (Fig. 8 *F*). The tubular assembling of N-25 mutant were less than wild-type (Fig. 8 *E*). Among them many oval structures with a hollow core in various diameters were observed (Fig. 8 *D*). These results imply a rigid and ordered packing of δ-crystallin aggregates, similar to the paracrystal of argininosuccinate lyase, which showed a hollow tubular structure with helical arrangement (35).

DISCUSSION

δ-Crystallin is a structural protein of avian eye lens that exists as tetramers. This lens protein then self-assembles and/or packs with other crystallins in high concentration in the limited space of lens cell while remaining soluble to fulfill its biological function. To explore packing of this protein in lens tissue, we studied the folding pathways of δ-crystallin (10,11). In previous reports we proposed a multistep unfolding pathway of GdmCl denaturation involving dissociation of tetramer to dimers and then to monomers, followed by the formation of a molten globular intermediate, and finally collapse of the protein structure. In this study, we have demonstrated that this process is fully reversible upon dilution of GdmCl. However, final assembling of two dimers to the tetramer has a kinetic barrier that leads to protein aggregate. The folding reversibility of δ-crystallin can be sensitively probed by intrinsic tryptophan fluorescence. In δ-crystallin, there are two tryptophans residues: W74, located at the solvent accessible N-terminus; and W169, buried in the helix bundle of domain 2. Dilution of 5 M-GdmCl unfolded δ-crystallin initiates the refolding process. Nonetheless, hysteresis behavior was observed in the refolding process when GdmCl concentrations were <1 M. The single tryptophan mutant protein reflects the environment variation surrounding the area where they located. The unfolding/refolding curves of W74 were not identical with each other implying that the solvent accessible N-terminus of domain 1 cannot properly refold. On the contrary, the completely reversible unfolding/refolding process for W169 indicates that the helix bundle of domain 2 is essentially reversible. In summary, refolding of the GdmCl-denatured

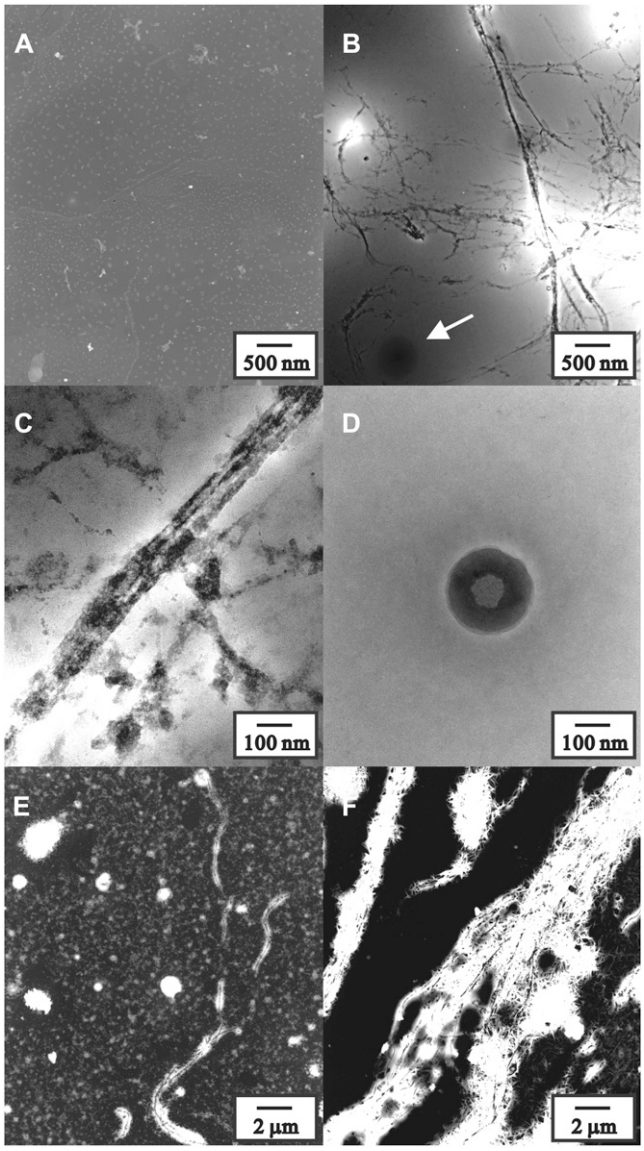

FIGURE 8 Transmission electron micrographs of δ-crystallin aggregates. The equilibrium denatured wild-type proteins were diluted in 50 mM Tris-Cl, pH 7.5, for 0 min (*A*), 6 h (*B–D*), and overnight (*E* for N-25 mutant and *F* for wild-type), respectively, and then negatively stained. The final protein concentration was 0.047 mg/ml for panels *A–D* and 0.19 mg/ml for panels *E* and *F*. Bars represent 500 nm for panels *A* and *B*, 100 nm for panels *C* and *D*, and 2 μm for panels *E* and *F*, respectively. Panel *D* is the enlarged image for the area shown by arrow in *B*.

δ-crystallin can restore the secondary structure but the tertiary structure was only partly reversible.

The hysteresis behavior in the unfolding/refolding process for δ-crystallin is identical to that observed in transthyretin (30) and may be explained by a similar mechanism. That is, a kinetic barrier exists in the reassembly transition between dimers and tetramers, and thus it is different from dissociation of tetramers into dimers. Dissociation of tetramers into monomers of δ-crystallin started at around 1 M GdmCl with transient formation of dimeric form (11). In contrast refolding of monomers and assembly into dimers is instantaneous, but further assembly of two dimers into the tetramer is delayed (Figs. 4 and 5). The observed hysteresis behavior appears to result from this kinetic barrier to the reconstitution of the folded tetramer. Presumably the observed behavior results from the need to correctly orientate the surfaces of the two dimers such that the weak noncovalent interactions required for assembly into the tetramer can occur (36). Aggregates are formed by a competing process in which dimers interact nonspecifically.

The kinetic refolding intermediate that leads to dimer, tetramer, or aggregation is supposed to be a molten globule state. The secondary structure of this intermediate state should be similar to the native state after refolding, whereas the conformation of domain 1 is not. Several hydrophobic patches of this folding intermediate may still be unburied and hence favor oligomerization or aggregation. We proposed several types of association of the molten globule state (Fig. 9), including native-like tetramer formation through double dimer assembly, or an alternative nucleus-seeded aggregation that has the propensity to propagate as high molecular weight aggregates and eventually precipitate.

N-terminal truncation hampers the refolding of δ-crystallin, particularly at the final tetramer assembly stage. In our previous studies, we have demonstrated that removal of the first N-terminal 25 residues have profound influence on the dimer assembly and stabilization of tetrameric conformation (9). The N-25 mutant is less resistant to unfolding by GdmCl. Interestingly, the dimer was the major species observed during the kinetically traced refolding of the N-25 mutant. Obviously, N-terminus truncation increases the uphill free-energy landscape for the dimer-tetramer assembly. Interactions arisen from N-terminal region are one of the key interactions that enable tetramer formation and allow the kinetic barrier to be overcome. Since an uphill free-energy landscape was created due to the slow assembly of two dimers, the protein could be trapped in a different low energy conformation that progresses into larger molecular weight aggregates.

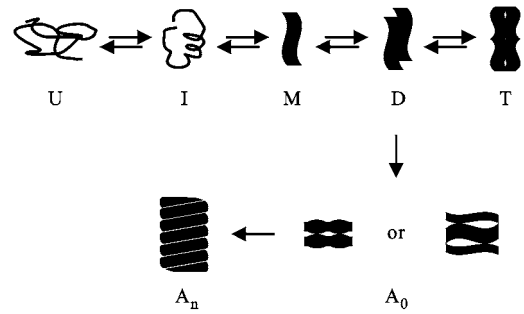

FIGURE 9 A working model proposed for unfolding, refolding, and aggregation pathways of goose δ-crystallin. Labels used represent: T, tetramer; D, dimer; M, molten globule monomer, I, intermediate, U, unfolded monomer, A_0, nuclear aggregate; A_n, high molecular weight aggregate.

Aggregates of δ-crystallin have regular structure and may propagate via a nucleation mechanism. The formation of aggregate particles requires a delay time for seed production. This process is protein concentration dependent with the apparent reaction order of 4.7 implying that four or five monomers are associated to form the nucleus in the initial stage. Other monomers then added to the nucleus or several nuclei assembly to yield high molecular weight aggregates (Fig. 9) (31). These aggregates can be sensitively investigated by ThT and CR binding. ThT has been demonstrated to be able to stain the regular structure of the high molecular weight aggregates having amyloid-like characteristics (37). However, unlike the common cross-β-sheet macromolecular assembly found in amyloidal fibril, δ-crystallin aggregates were found to have a regular helical arrangement. TEM clearly revealed the tubular shape of δ-crystallin aggregates. In a time-dependent manner, δ-crystallin aggregates grow from irregular spherical dark aggregates to unbranched tubules, followed by twisting these tubules into a bundle. Several bundles then assemble into loosely packed bundles.

The morphology of goose δ-crystallin is similar to the paracrystal of argininosuccinate lyase, which has a hollow tubular structure with a helical arrangement (35). A supermolecular structure was also reported for turkey δ-crystallin under crystallization conditions around neutral pH (38). The crystal structure contains three and a half tetramers in the asymmetric unit, with a tetrahedral shape in the tetrameric structure (6). The tetramers associated into a novel packing of continuous helices, and then several helices were assembled into an approximately hexagonal close-packed array in the crystal. In the nucleation mechanism, the goose δ-crystalline aggregates arise from association of four partially unfolded monomers to form the seeding nucleus, which then extend into continuous helices with a different diameter to that observed with ASL or turkey δ-crystallin.

These results provide an explanation for the posttranslational modification occurring in lens proteins during aging. The kinetic barrier prevents reconstitution of the stable soluble tetramer and the partially unfolded or damaged lens protein then diverted to form aggregates (cataracts). The chaperone activity of α-crystallin, the ubiquitous protein component in eye lens, thus becomes pivotal in the maintenance of lens transparency (39). Our results clearly demonstrated the protective effect of α-crystallin against aggregation. However, in contrast to the proposed interaction of α-crystallin with the N-terminal arm of δ-crystallin to compete for self-association of δ-crystallin (38), we found a similar protective effect for the N-terminal truncated δ-crystallin by α-crystallin suggesting other possible protein-protein interactions may be involved.

In conclusion, we have demonstrated a reversible unfolding-refolding for the GdmCl denaturation of goose δ-crystallin involving a molten globule state. This folding intermediate is at the crossroads of diverse subunit association pathways. The kinetically unfavorable double dimer assembly favors the alternative aggregate formation pathway, which led to a helical tubule structure. The N-terminal segment of δ-crystallin was confirmed to be critical for double dimer assembly and is also involved in aggregate formation.

We thank Dr. H. C. Chang for the use of CD spectroscopy in the Institute of Biological Chemistry, Academia Sinica. We also thank Dr. M. D. Lloyd (University of Bath, UK) for reading this manuscript before publication and Dr. G. G. Chang (National Yang-Ming University, Taiwan) for helpful discussions.

This study was supported financially by the National Science Council (NSC 94-2113-M-016-001 to H.-J.L.).

REFERENCES

1. Wistow, G. J., and J. Piatigorsky. 1988. Lens crystallins: the evolution and expression of proteins for a highly specialized tissue. *Annu. Rev. Biochem.* 57:479–504.
2. Wistow, G. J., and J. Piatigorsky. 1990. Gene conversion and splice-site slippage in the argininosuccinate lyases/delta-crystallins of the duck lens: members of an enzyme superfamily. *Gene*. 96:263–270.
3. Piatigorsky, J. 1992. Lens crystallins. Innovation associated with changes in gene regulation. *J. Biol. Chem.* 267:4277–4280.
4. Wistow, G. J. 1993. Lens crystallins: gene recruitment and evolutionary dynamism. *Trends Biochem. Sci.* 18:301–306.
5. Piatigorsky, J., and G. J. Wistow. 1991. The recruitment of crystallins: new functions precede gene duplication. *Science.* 252:1078–1079.
6. Simpson, A., O. Bateman, H. Driessen, P. Lindley, D. Moss, S. Mylvaganam, E. Narebor, and C. Slingsby. 1994. The structure of avian eye lens delta-crystallin reveals a new fold for a superfamily of oligomeric enzymes. *Nat. Struct. Biol.* 1:724–734.
7. Turner, M. A., A. Simpson, R. R. McInnes, and P. L. Howell. 1997. Human argininosuccinate lyase: a structural basis for intragenic complementation. *Proc. Natl. Acad. Sci. USA*. 94:9063–9068.
8. Sampaleanu, L. M., F. Vallee, C. Slingsby, and P. L. Howell. 2001. Structural studies of duck delta 1 and delta 2 crystallin suggest conformational changes occur during catalysis. *Biochemistry*. 40:2732–2742.
9. Lee, H. J., Y. H. Lai, S. Y. Wu, and Y. H. Chen. 2005. The effect of N-terminal truncation on double dimer assembly of goose δ-crystallin. *Biochem. J.* 392:545–554.
10. Lee, H. J., and G. G. Chang. 2000. Guanidinium chloride induced reversible dissociation and denaturation of duck δ2-crystallin. *Eur. J. Biochem.* 267:3979–3985.
11. Lee, H. J., S. W. Lu, and G. G. Chang. 2003. Monomeric molten globule intermediate involved in the equilibrium unfolding of tetrameric duck δ2-crystallin. *Eur. J. Biochem.* 270:3988–3995.
12. Lee, H. J., Y. H. Lai, Y. T. Huang, C. W. Huang, Y. H. Chen, and G. G. Chang. 2006. Critical role of tryptophanyl residues in the conformational stability of goose δ-crystallin. *Exp. Eye Res.* 83:658–666.
13. Jaenicke, R. 1998. Protein self-organization in vitro and in vivo: partitioning between physical biochemistry and cell biology. *Biol. Chem.* 379:237–243.
14. Shinde, U. P., J. J. Liu, and M. Inouye. 1997. Protein memory through altered folding mediated by intramolecular chaperones. *Nature*. 389: 520–522.
15. Kosinski-Collins, M. S., and J. King. 2003. In vitro unfolding, refolding, and polymerization of human γD crystallin, a protein involved in cataract formation. *Protein Sci.* 12:480–490.
16. Li, S., J. H. Bai, Y. D. Park, and H. M. Zhou. 2006. Capture of monomeric refolding intermediate of human muscle creatine kinase. *Protein Sci.* 15:171–181.
17. Zettlmeissl, G., R. Rudolph, and R. Jaenicke. 1979. Reconstitution of lactic dehydrogenase. Noncovalent aggregation vs. reactivation. 1.

Physical properties and kinetics of aggregation. *Biochemistry*. 18: 5567–5571.

18. Rudolph, R., G. Zettlmeissl, and R. Jaenicke. 1979. Reconstitution of lactic dehydrogenase. Noncovalent aggregation vs. reactivation. 2. Reactivation of irreversibly denatured aggregates. *Biochemistry*. 18: 5572–5575.
19. Wiseman, R. L., E. T. Powers, and J. W. Kelly. 2005. Partitioning conformational intermediates between competing refolding and aggregation pathways: insights into transthyretin amyloid disease. *Biochemistry*. 44:16612–16623.
20. Stefani, M., and C. M. Dobson. 2003. Protein aggregation and aggregate toxicity: new insights into protein folding, misfolding diseases and biological evolution. *J. Mol. Biol*. 81:678–699.
21. Sipe, J. D., and A. S. Cohen. 2000. Review: history of the amyloid fibril. *J. Struct. Biol*. 130:88–98.
22. Jahn, T. R., and S. E. Radford. 2005. The Yin and Yang of protein folding. *FEBS J*. 272:5962–5970.
23. Chang, G. G., H. J. Lee, and R. H. Chow. 1997. pH-Induced reversible dissociation of tetrameric duck lens delta-crystallin. *Exp. Eye Res*. 65: 653–659.
24. Bradford, M. M. 1976. A rapid and sensitive method for the quantitation of microgram quantities of protein utilizing the principle of protein-dye binding. *Anal. Biochem*. 72:248–254.
25. Sanchez del Pino, M. M., and A. R. Fersht. 1997. Nonsequential unfolding of the α/β barrel protein indole-3-glycerol-phosphate synthase. *Biochemistry*. 36:5560–5565.
26. Kelly, S. M., and N. C. Price. 1997. The application of circular dichroism to studies of protein folding and unfolding. *Biochim. Biophys. Acta*. 1338:161–185.
27. Fersht, A. 1999. Structure and mechanism in protein science: a guide to enzyme catalysis and protein folding. W. H. Freeman and Company, New York.
28. Klunk, W. E., J. W. Pettegrew, and D. J. Abraham. 1989. Two simple methods for quantifying low-affinity dye-substrate binding. *J. Histochem. Cytochem*. 37:1293–1297.
29. Naiki, H., K. Higuchi, M. Hosokawa, and T. Takeda. 1989. Fluorometric determination of amyloid fibrils *in vitro* using the fluorescent dye, thioflavine T. *Anal. Biochem*. 177:244–249.
30. Lai, Z. H., J. McCulloch, H. A. Lashuel, and J. W. Kelly. 1997. Guanidine hydrochloride-induced denaturation and refolding of transthyretin exhibits a marked hystersis: equilibria with high kinetic barriers. *Biochemistry*. 36:10230–10239.
31. Hofrichter, J., P. D. Ross, and W. A. Eaton. 1974. Kinetic mechanism of deoxyhemoglobin S gelation: a new approach to understanding sickle cell disease. *Proc. Natl. Acad. Sci. USA*. 71:4864–4868.
32. Khurana, R., V. N. Uversky, L. Nielsen, and A. L. Fink. 2001. Is Congo red an amyloid-specific dye? *J. Biol. Chem*. 276:22715–22721.
33. Merlini, G., and V. Bellotti. 2003. Molecular mechanisms of amyloidosis. *N. Engl. J. Med*. 349:583–596.
34. Ross, C. A., and M. A. Poirier. 2004. Protein aggregation and neurodegenerative disease. *Nat. Med*. 10:S10–S17.
35. Dales, S., I. T. Schulze, and S. Ratner. 1971. Tubular organization of crystalline argininosuccinase. *Biochim. Biophys. Acta*. 229:771–778.
36. Milla, M. E., B. M. Brown, C. D. Waldburger, and R. T. Sauer. 1995. P22 Arc repressor: transition state properties inferred from mutational effects on the rates of protein unfolding and refolding. *Biochemistry*. 34:13914–13919.
37. Khurana, R., C. Coleman, C. Ionescu-Zanetti, S. A. Carter, V. Krishna, R. K. Grover, R. Roy, and S. Singh. 2005. Mechanism of thioflavin T binding to amyloid fibrils. *J. Struct. Biol*. 151:229–238.
38. Simpson, A., D. Moss, and C. Slingsby. 1995. The avian eye lens protein δ-crystallin shows a novel packing arrangement of tetramers in a supramolecular helix. *Structure*. 3:403–412.
39. Horwitz, J. 2003. Alpha-crystallin. *Exp. Eye Res*. 76:145–153.